

Supporting Information for

Ultra-Antireflective Electrodeposited Plasmonic and PEDOT Nanocone Array Surfaces

*Han Wai Millie Fung, Seulgi So, Kellen Kartub, Gabriel Loget† and Robert M. Corn**

Department of Chemistry and Department of Biomedical Engineering, University of California-Irvine, Irvine, CA 92697, USA.

†Present Address: Institut des Sciences Chimiques de Rennes, UMR 6226 CNRS, Université de Rennes 1, Campus de Beaulieu, 35042 Rennes Cedex, France.

*Robert M. Corn: rcorn@uci.edu

Experimental Details for Simulated %R Measurements for Nanocone Arrays

The simulated %R measurements were obtained using 11-phase Fresnel calculations, where $n_1 =$ air, $n_{11} =$ bulk Au or ZnO-Au, and $n_2, n_3, \dots, n_{10} =$ the effective refractive index calculated by averaging the refractive indices of air and the nanocone structure as a function of the distance away from the bottom of the nanocone. For Au, n_{11} at various λ was referenced from values reported in literature. To calculate the real part of n_2, n_3, \dots, n_{10} , the following formula was used:

$$n_{xreal} = n_{xreal} = n_{xreal+1} + \left(\frac{1-n_{11real}}{10}\right), \text{ where } 2 < x < 10$$

To calculate the imaginary part of n_2, n_3, \dots, n_{10} , the following formula was used:

$$n_{xim} = n_{11im} e^{-\left(\frac{11-x}{7}\right)}, \text{ where } 2 < x < 10$$

For ZnO-Au, n_{11} at various λ was modeled using the refractive index of ZnO reported in literature. However, we also combined the imaginary part of Au's refractive index to model the

absorptive nature of the ZnO-Au nanocone arrays (e.g., at 600 nm, $n_{\text{Au}} = 0.24 + 3.10i$, $n_{\text{ZnO}} = 2.00 + 0i$, and ZnO-Au is modeled using $n_{\text{ZnO-Au}} = 2.00 + 3.10i$). To calculate the real and imaginary parts of n_2, n_3, \dots, n_{10} for the ZnO-Au nanocone arrays, the same formulas listed above were used. Other important parameters for the Fresnel calculations include setting the film height for each phase from n_2, n_3, \dots, n_{10} to 100 nm, and setting the angle of incidence to 8° .

Figure S1

Electrochemical characterization of the formation of the nanostructured ZnO thin film via electrodeposition.

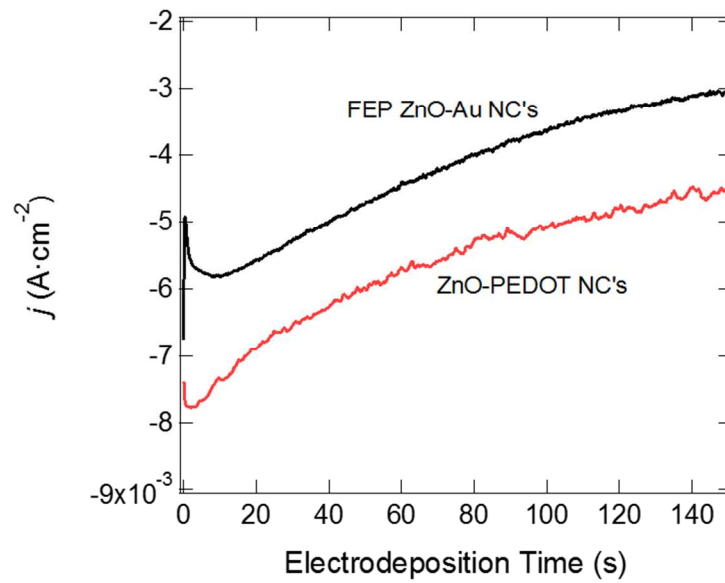


Figure S2

XRD analysis of the ZnO-coated nanocone arrays indicates a wurzite structure with polycrystalline ZnO growing primarily in the $\langle 002 \rangle$ direction.

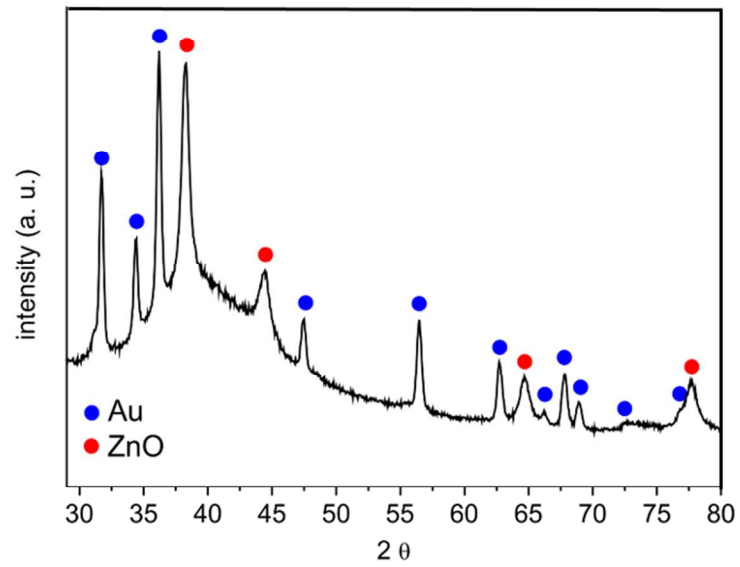


Figure S3

XPS analysis confirming the presence of ZnO on the surface of the FEP ZnO-Au nanocone arrays and the ZnO-PEDOT nanocone arrays. a) indicates the presence of both Zn $2p_{3/2}$ and Zn $2p_{1/2}$ peaks, while b) indicates the presence of the O 1s peak.

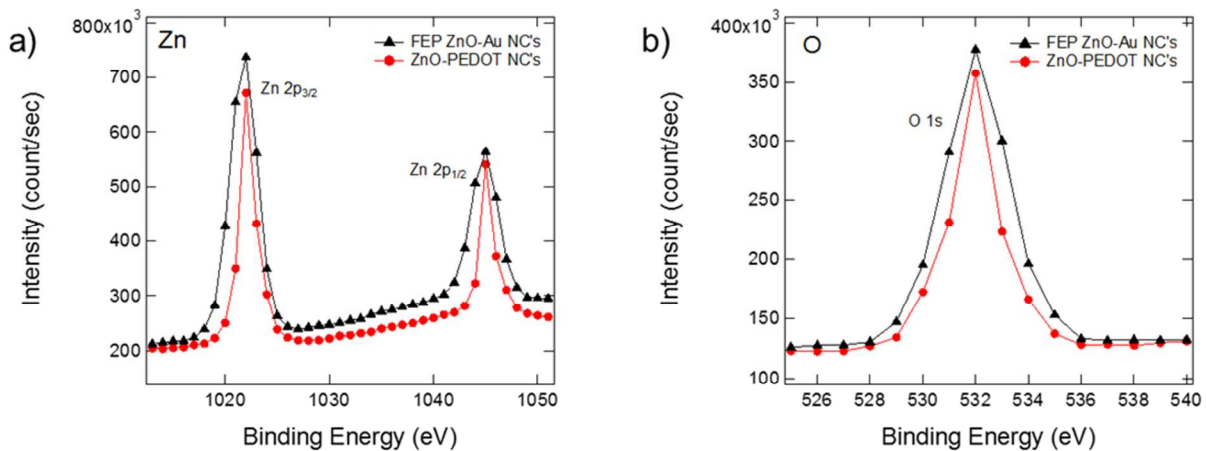


Figure S4

a) UV-Vis absorbance spectra of methylene blue in the presence of the ZnO-coated nanocone array catalyst. The inset shows that the methylene blue is fully degraded after 14 minutes, thus losing all its color. b) Confirmation of the increased surface area of the ZnO nanocone arrays via their improved photocatalytic performance in the degradation of methylene blue dye. SEM images of c) the planar ZnO thin film surface and d) the ZnO nanocone arrays used in the methylene blue degradation. For the planar ZnO thin film, the ZnO crystals are packed tightly together, reducing the surface roughness factor compared to the periodic ZnO-coated nanocone arrays.

